東邦大学学術リポジトリ
Toho University Academic Repository

タイトル	Dose distribution evaluation of the internal target volume in stereotactic body radiotherapy for lung cancer
別タイトル	肺癌に対する体幹部定位放射線治療における体内標的体積への線量分布の評価
作成者（著者）	清水, 友理
公開者	東邦大学
発行日	2016.07
掲載情報	東邦大学大学院医学研究科 博士論文. 3. p.33-44.
資料種別	学位論文
内容記述	主査 : 澁谷和俊 / タイトル : Dose distribution evaluation of the internal target volume in stereotactic body radiotherapy for lung cancer /著者 : Yuri Shimizu, Naoya Saotome, Masahiko Futaguchi, Shinobu Kumagai, Atsuro Terahara /掲載誌 : Toho Journal of Medicine /巻号・発行年等 : 2(2):33-44, 2016 /本文ファイル: 出版者版
著者版フラグ	ETD
報告番号	32661甲第808号
学位授与年月日	2016.07.29
学位授与機関	東邦大学
DOI	info:doi/10.14994/tohojmed.2016.005
その他資源識別子	https://mylibrary.toho-u.ac.jp/webopac/TD52013241
メタデータのＵＲＬ	https://mylibrary.toho-u.ac.jp/webopac/TD22242098

Original Article

Dose Distribution Evaluation of Internal Target Volume in Stereotactic Body Radiotherapy for Lung Cancer

Yuri Shimizu[1)*] Naoya Saotome[2)] Masahiko Futaguchi[1, 3)]
Shinobu Kumagai[4)] and Atsuro Terahara[1)]

[1)]Department of Radiology (Omori), School of Medicine, Faculty of Medicine, Toho University
[2)]Department of Research Center for Charged Particle Therapy, National Institute of Radiological Sciences
[3)]Department of Radiology, University of Tokyo Hospital
[4)]Department of Radiology, Teikyo University Hospital

ABSTRACT

Background: Three-dimensional computed tomography (3DCT) is used in planning stereotactic body radiotherapy (SBRT) for lung cancer (3D plan). To accurately evaluate dose distribution for internal target volume (ITV), we recalculated a 3D plan using all breathing phases for four-dimensional computed tomography (4DCT).

Methods: The study included 8 patients with one tumor each who underwent SBRT for stage I lung cancer. After performing free-breathing 3DCT, 4DCT was performed. The prescription dose in the 3D plan was 48 Gy/4 fr or 56 Gy/7 fr for the ITV mean in 3DCT. We recalculated 3D plan radiation conditions for each breathing phase of 4DCT and accumulated dose distributions for all breathing phases (4D plan) with deformable image registration. A dose-volume histogram and a dose distribution map were used to evaluate dose distribution.

Results: For all patients, the maximum difference between the 3D and 4D plans for the minimum dose applied to 2% of the ITV or ITV mean was 2.6% and 1.7% respectively. For the 3 patients who exhibited substantial respiratory movement of the tumor, the dose distribution changed in accordance with the observed differences in tumor shadows for registered 4DCT and primary 3DCT during dose accumulation, and the difference between plans for the minimum dose applied to 98% of the ITV was relatively large, −6.7% to 2.9%.

Conclusions: We used 4D plan evaluation to confirm that the intended doses were applied to the ITV using the 3D plan. When using a 4D plan with deformable image registration to evaluate the dose distribution of a 3D plan, the selection of primary computed tomography for dose accumulation is important.

Toho J Med 2 (2): 33–44, 2016

KEYWORDS: stereotactic body radiotherapy, stage I lung cancer, internal target volume, four-dimensional computed tomography (4DCT), deformable image registration

1) 6–11–1 Omorinishi, Ota, Tokyo 143–8541, Japan
2) 4–9–1 Anagawa, Inage, Chiba 263–8555, Japan
3) 7–3–1 Hongo, Bunkyo, Tokyo 113–8655, Japan
4) 2–11–1 Kaga, Itabashi, Tokyo 173–8606, Japan
*Corresponding Author: tel: +81–(0)3–3762–4151
e-mail: yuri.shimizu@med.toho-u.ac.jp
DOI: 10.14994/tohojmed.2016.005
Received Feb. 10, 2016: Accepted Mar. 15, 2016
Toho Journal of Medicine 2 (2), June 1, 2016.
ISSN 2189–1990, CODEN: TJMOA2

Previous reports indicate that the local control rate of stereotactic body radiotherapy (SBRT) for stage I non-small cell lung cancer is the same as that for standard surgical treatment.[1–4] Furthermore, the 5-year local recurrence-free survival rate of SBRT for stage I non-small cell lung cancer (approximately 69%) is better than that of normal fractionated radiotherapy.[5] The Japan Clinical Oncology Group 0403 trial (JCOG-0403) reported that the 3-year survival rate of SBRT for stage IA non-small cell lung cancer was 76.0% for operable cases and 59.9% for inoperable cases.[6]

Respiratory movement is an important variable in determining internal margins for chest organs. Patients with lung cancer exhibit considerable respiratory movement, reportedly greater than 0.5 cm in a free-breathing state, and some reports indicate that it can reach 2 cm.[7, 8] When performing radiotherapy in lung cancer cases, it is important to understand tumor respiratory movement in order to apply radiation to the target accurately, without increasing the risk of adverse events in surrounding organs. When applying radiation in a free-breathing state, target settings that consider respiratory movement are needed.[9–13] SBRT requires highly precise establishment of tumor location during treatment and target settings, as it involves applying large doses of radiation in one fraction, such as 48 Gy/4 fr or 56 Gy/7 fr.

In recent years, the appearance of four-dimensional computed tomography (4DCT) has meant that three-dimensional (3D) respiratory movement can now be more accurately and easily understood than with conventional 3D computed tomography (3DCT).[14, 15] In free-breathing 4 DCT, respiratory waveforms are acquired during simultaneous acquisition of CT images, making it possible to correlate images with breathing phases and subdivide one respiratory cycle into, typically, 8 to 15 phases. In this manner, images can be assembled chronologically and reconstructed for each breathing phase.[16] When performing free-breathing imaging, 3DCT can only yield images of particular breathing phases and cannot be used to assess tumor movement accompanying breathing. In contrast, 4DCT can be used to acquire images showing actual tumor movement accompanying breathing over one respiratory cycle. Furthermore, as compared with 3DCT, 4DCT images have fewer motion artifacts of the tumor and surrounding organs. Therefore, 4DCT is useful in evaluating gross tumor volume (GTV) and clinical target volume (CTV). When GTV and CTV on 4DCT data are used as a reference, dose prescriptions can now be made in accordance with more accurately contoured internal target volume (ITV) and planning target volume (PTV).[14, 17]

In clinical practice, SBRT treatment plans for early-stage primary lung cancer are created after dose calculation using data such as free-breathing 3DCT or average intensity projection (AIP) images derived from 4DCT (3D plan). Dose distribution calculated using 3DCT may differ from the actual dose distribution, because this treatment involves irradiation of tumors exhibiting respiratory movement. By accumulating all breathing phases on 4DCT (4D plan), values closer to the actual dose distribution applied with GTV or CTV can be calculated. However, it takes time to construct a 4D plan and can be difficult to introduce clinically. Because the dose distribution in these stereotactic treatment plans is commonly not uniform, low-dose regions in one breathing phase can often be compensated for by high doses in another phase. Thus, comparing 4D dose distributions in each individual phase is not an appropriate method of evaluating 4D dose. To evaluate 4D dose distribution, the doses for each breathing phase must be accumulated. Because respiratory movement alters organ shape, deformable image registration (DIR) is required in order to increase the accuracy of dose accumulation. DIR is intensity-based and is performed in accordance with the contrast between voxels on CT. DIR can be used to develop a method of accumulating 4D dose distribution while maintaining dose-to-voxel correspondence. This makes it possible to perform a dose accumulation that accounts for movement.[18–20] However, DIR requires complicated processing, and no specific method has been established; its use is therefore currently restricted to research applications.

Previous studies of 4D dose distribution in SBRT for early-stage primary lung cancer confirmed that an ITV dose calculated for one phase of 4DCT or AIP images derived from 4DCT was a good approximation of GTV dose and CTV dose calculated for all phases of 4DCT by dose accumulation. However, some studies reported that 3D dose at the PTV margin underestimated the 4D dose of GTV and CTV.[21–23] PTV has setup margins of approximately 5 mm around the ITV. In lung cancer therapy, the PTV has a larger area of normal lung shadows surrounding the tumor, as compared with ITV. The dose for normal lung areas is lower than that for tumor shadows, because the CT density of normal lung areas is lower than that of tumor shadows. Therefore, dose distribution can be con-

siderably lower in the PTV margin than in the ITV. Furthermore, SBRT treatment plans for lung cancer often stipulate a dose prescription for ITV on free-breathing 3DCT in a clinic. In addition, regarding ITV dose, previous reports evaluated the results of doses calculated during one phase on 4DCT or AIP images derived from 4DCT.[21–23] Therefore, we evaluated differences in ITV dose between 4D and 3D plans. To evaluate a dose distribution for the ITV that is closer to the actual state, we recalculated the 3D plan using all breathing phases on 4DCT.

Materials and Methods

Patients

The subjects in this study were 8 patients who underwent SBRT at the Department of Radiation Oncology, Toho University Oomori Medical Center, Japan, between June 2013 and May 2014 after being diagnosed with T1-2aN0M0 stage I primary lung cancer, according to the seventh edition of the International Union Against Cancer (UICC) Tumor-Node-Metastasis (TNM) classification. Physicians in the department of thoracic surgery determined patient eligibility for surgery. However, surgery was contraindicated for the present patients because of factors such as performance status, age, and cardiopulmonary function. Histological analysis of biopsy specimens did not yield a definitive diagnosis for any of the present patients. All diagnoses were instead based on clinical course, cytological results, histological diagnosis results, and diagnostic imaging.

Because this study involved treatment plans and 4DCT images for evaluating dose distribution, the Toho University Omori Medical Center research ethics board approved the use of patient data (approval no. 27–204). However, because this study did not involve any actual intervention in treatment, patient informed consent was not required.

Image acquisition

CT was performed by obtaining consecutive free-breathing 3DCT and 4DCT images. The patient was placed in a dorsal position, with both arms elevated toward the head using arm supports (ESFORM; Engineering System Co., Ltd., Matsumoto, Japan). The trunk was fixed using an individually shaped body cast, a trunk fixation plate, and a suction-type fixation cushion (all by ESFORM). CT imaging was performed using a CT scanner with a 16-row detector (Aquilion™ LB; Toshiba Medical Systems Corp., Otawara, Japan). The 3DCT imaging was performed using the helical scan method. After 3DCT imaging, we performed 4DCT imaging, also with the helical scan method. The 4DCT imaging conditions were 120 kVp, 10 to 50 mA, 0.5-s gantry rotation time, 0.8 to 1.2 pitch (depending on respiration rate), 1.0-mm slice collimation, 2-mm slice thickness, and a 512 × 512 matrix. Using a detection sensor (AZ-733V; Anzai Medical Co., Ltd, Tokyo, Japan) that depicts abdominal movement as respiratory waveforms, we acquired respiratory waveforms simultaneously with 4DCT imaging. Each respiratory cycle was divided into 10 phases, and image data were rearranged into the respective breathing phases, after which 4DCT images were reconstructed.

SBRT planning

Data from 3DCT and 4DCT imaging were transferred to Pinnacle software version 9.2–9.6 (Philips, Amsterdam, The Netherlands), and the ITV was contoured on 3DCT to include all of the CTV for each 4DCT phase. Contouring was performed by an experienced radiation oncologist. Treatment planning was conducted on 3DCT using Pinnacle software. Mean dose prescription to ITV was set at 48 Gy/4 fr. For one patient with a tumor adjacent to the pulmonary hilum, the dose prescription was set at 56 Gy/7 fr, to reduce the dose per fraction and thereby lower the risk of adverse events in surrounding organs. Planning was conducted with the objective of distributing at least 95% of the prescribed dose to 98% of the ITV. Fixed multiport irradiation with a non-coplanar beam was performed, and 6 to 11 beams were used. A 4-megavolt (MV) X-ray device was used for one patient, and a 6-MV X-ray was used for the other 7 patients. Dose calculation was performed with the collapsed cone convolution superposition algorithm, with density correction and a calculation grid size of $2 \times 2 \times 2\ mm^3$.

Registration and dose accumulation

Although the entire lung field is contained in 3DCT, and imaging includes the entire range of beam penetration, 4DCT only scans around the target on the cranial/caudal axis. Therefore, the cranial and caudal data required for dose calculation on 4DCT were supplemented with 3DCT, using an in-house program. Next, dose calculation was conducted for each 4DCT breathing phase, using the Pinnacle software and the actual irradiation conditions on the 3D plan, such as the shape of the multi-leaf collimator, isocenter position, and the monitor unit for each beam. Using advance verification, we confirmed that the same CT-to-density conversion table could be used in dose calculation

for 3DCT and 4DCT. We then constructed dose distribution maps for 4DCT in each breathing phase.

Dose distribution for each breathing phase was transmitted to the MIM Maestro™ software suite version 6.1.7 (MIM Software Inc., Cleveland, OH, USA), radiotherapy support system, and the dose distribution for all breathing phases was accumulated. Dose accumulation was calculated using an existing default accumulation program in the MIM Maestro™ software and the DIR. The primary CT for accumulation was 3DCT, and 10 dose distribution sets for each breathing phase of 4DCT were sequentially layered on 3DCT. Because each breathing phase was equally divided by duration in the 4DCT reconstruction process, the chronological weight (probability density function) of each breathing phase was considered equal in dose accumulation.

Dose distribution evaluation

The evaluation target was ITV on 3DCT. Accumulated dose distribution was analyzed after converting dose distribution to numerical terms, using a dose–volume histogram (DVH), and visual evaluation was performed using dose distribution maps. The items evaluated were mean dose applied to the ITV, minimum dose distributed in 2% of ITV (D2) as an approximation of maximum dose, minimum dose distributed in 98% of ITV (D98) as an approximation of minimum dose, minimum dose distributed to 95% of ITV (D95), ITV homogeneity index (HI), and ITV conformity index (CI). HI was calculated as "minimum dose (Dmin)/maximum dose (Dmax)". CI was calculated as "volume to which minimum ITV dose is applied/ITV".

To determine how dose accumulation results changed when primary CT differed, we defined the accumulated dose for all breathing phases with the maximum expiration phase in 4DCT as the primary CT. We also analyzed how isodose curves changed when the DIR of only one phase was performed. Furthermore, we examined differences in tumor shadows between 3DCT and 4DCT.

Verification of DIR accuracy

During dose accumulation, DIR of each breathing phase in 4DCT and 3DCT was performed. The DIR algorithm is derived theoretically and is known to differ from actual target deformation. Although previous reports have confirmed the precision of DIR, no standard method has been established, although a few previous reports implemented the MIM DIR workflow precision verification that we used here.[24–26] We verified DIR precision using the method reported by Balik et al.[27] Briefly, an experienced radiotherapist contoured the CTV on 3DCT as manual contours. In this study, we assumed no CTV margin around the GTV in principle and labeled the manually contoured CTV as the contour. On the basis of the CTV contours on 4DCT, CTV was contoured automatically with MIM DIR workflow on 3DCT as warped contours. To verify DIR precision, we measured the Dice similarity index for the warped contours and manual contours.[28] The Dice similarity index measures the overlap of 2 segmentations, A and B, and is defined as

$$\frac{2|A \cap B|}{|A|+|B|}.$$

The closer the results calculated for each calculation formula are to one, the greater the precision. In addition, we measured the distance from the manual contour central coordinate to the warped contour central coordinate. Central coordinates for each type of contour were calculated using an existing MIM function.

Results

Table 1 shows the characteristics of the 8 patients. For the 3 axes, the amount of movement tended to be greatest on the cranial/caudal axis. Pulmonary emphysema was present in cases 4 and 8.

Dose distribution

Table 2 shows the mean values for ITV D2, mean dose, D95, and D98 for the 3D and 4D plans. Values for case 2, for which a treatment dose of 56 Gy/7 fr was prescribed, were calculated after converting the prescription dose to 48 Gy/4 fr in Table 2. The mean overall HI was 1.15 (range: 1.06–1.31) for the 3D plans and 1.18 (range: 1.07–1.33) for the 4D plans. The mean overall CI was 3.36 (range: 1.37–4.85) for the 3D plans and 3.92 (range: 3.08–5.41) for the 4D plans. Dose differences obtained by subtracting the 3D plan dose from the 4D plan dose are shown as percentages of the 3D plan dose in Table 3. Fig. 1 shows box plots of the data from Table 3. There was little difference in mean dose between plans, but the differences were greater for the other dose variables. The mean dose for the 4D plan tended to be equal or greater than that of the 3D plan. The dose variable that differed most between the 3D plans and 4D plans was D98 (Fig. 1), and the largest differences were seen for cases 1, 2, and 3 (Table 3).

DVH shape

Fig. 2 shows the DVH for the 3D and 4D plans of all patients. The DVH was scale-adjusted so that only high-dose parts were displayed. In cases 1 through 3, the differences

Table 1 Patient characteristics

Case No.	Age (years)	Tumor location	Tumor size (cm)	Tumor motion (cm)			
				SI	AP	LR	3D
1	76	L-LL	2.0	2.0	0.9	0.5	2.2
2	78	R-LL	1.5	1.2	<0.1	0.1	1.2
3	74	R-LL	1.5	0.8	0.5	0.2	0.9
4	78	R-LL	0.7	0.6	<0.1	<0.1	0.6
5	79	R-UL	3.0	<0.1	0.4	0.3	0.5
6	79	L-UL	1.5	0.5	0.2	0.1	0.5
7	78	R-UL	1.0	<0.1	<0.1	0.3	0.3
8	83	L-LL	1.8	<0.1	<0.1	0.1	0.1
Mean	—	—	1.6	1.0	0.5	0.2	0.9
Median	78						

No.: number, 3D: three-dimensional, SI: superior/inferior axis, AP: anterior/posterior axis, LR: left/right axis, L-LL: left lower lobe, R-LL: right lower lobe, R-UL: right upper lobe, L-UL: left upper lobe

Table 2 Mean ITV dose for the 8 patients

	D2 (Gy) Mean ± SD	Mean (Gy) Mean ± SD	D95 (Gy) Mean ± SD	D98 (Gy) Mean ± SD
3D plan	49.8 ± 0.8	48.0 ± 0.1	46.1 ± 1.3	45.6 ± 1.6
4D plan	50.3 ± 0.9	48.4 ± 0.2	46.0 ± 1.4	45.4 ± 1.8

The prescription dose for case 2 was 56 Gy/7 fr. The data in the table reflect the conversion of the prescription dose for case to 2 to 48 Gy/4 fr.
ITV: internal target volume, 3D: three-dimensional, 4D: four-dimensional, D2: minimum dose received by 2% of internal target volume, D95: minimum dose received by 95% of internal target volume, D98: minimum dose received by 98% of internal target volume, SD: standard deviation

Table 3 Dose difference of ITV between the 4D and 3D plans

Case No.	D2 (%)	mean dose (%)	D95 (%)	D98 (%)
1	2.0	0.0	−4.2	−6.7
2	1.3	1.7	2.2	2.9
3	2.6	1.0	−2.4	−5.3
4	0.5	0.7	1.3	1.4
5	0.9	0.9	1.3	0.9
6	0.9	0.4	−0.8	−0.9
7	0.2	1.1	1.3	1.3
8	0.6	0.5	0.1	−0.3

Dose differences are shown as percentages of the 3D plan dose.
ITV: internal target volume, No.: number, 3D: three-dimensional, 4D: four-dimensional, D2: minimum dose received by 2% of internal target volume, D95: minimum dose received by 95% of internal target volume, D98: minimum dose received by 98% of internal target volume

in DVH shape between the 3D and 4D plans were clearer than those for cases 4 through 8. In cases 1 and 3, the minimum 4D plan dose was exhibited lower than that of the 3D plan, and the volume in which the dose distribution was higher than the prescribed dose was larger in the 4D plan. In case 2, the curve for the 4D plan was shifted to the right, which indicates that the overall dose was higher for the 4D plan than for the 3D plan.

Isodose curves

Fig. 3A and B show the dose distributions for the 3D and 4D plans. The 4D plan isodose curves were more compressed on the cranial/caudal axis, as compared with those of the 3D plan, in cases 1 and 3. In case 2, the isodose curve was expanded on the cranial/caudal axis. Visually, there were no clear differences in the shapes of the isodose curves between the 3D and 4D plans in cases 4 through 8.

Dose accumulation with a different primary CT

Using 4DCT as the primary CT, we investigated accumulated dose. As compared with 3DCT, some dilation on the cranial/caudal axis was observed in case 1, cranial/caudal contraction was observed in case 2, and cranial/caudal dilation was observed in case 3 for isodose curves (Fig. 3C).

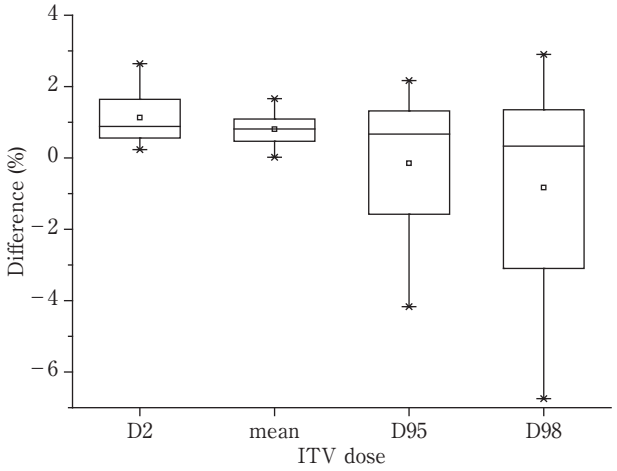

Fig. 1 Box plots of differences in ITV dose between the 4D and 3D plan. The box plots show differences in ITV dose as percentages of the corresponding 3D plan. The upper limits of the plots indicate upper adjacent values. The lower limits of the box plots indicate lower adjacent values. The squares inside the box plots indicate the mean.
ITV: internal target volume, D2: minimum dose received by 2% of internal target volume, D95: minimum dose received by 95% of internal target volume, D98: minimum dose received by 98% of internal target volume

One-phase DIR

Fig. 4A shows dose distribution in the 4DCT maximum inspiration phase. Fig. 4B shows the dose distribution on 3DCT, registered from dose distribution on a maximum inspiration phase 4DCT image using DIR. During DIR, the isodose curve changed to follow the movement of high-attenuation areas on the primary CT (Fig. 4).

Difference in tumor shadows

Fig. 5 shows free-breathing 3DCT and 4DCT during each breathing phase for cases 1, 2, and 3. In cases 1 and 3, tumor size was identical on 3DCT and 4DCT or slightly smaller on 3DCT. The tumor shadow movement accompanying respiration on 4DCT was more prominent than changes in size. In case 2, 3DCT tumor shadows were larger than those for each breathing phase on 4DCT (Fig. 5). Visually, there were no clear differences in tumor shadows between 3DCT and 4DCT in cases 4 through 8.

Verification of DIR precision

DIR precision verification was performed for cases 2 and 6. Case 2 represented the 3 patients with large cranial/caudal axis respiratory motion of the tumor. Case 6 represented the 5 patients with little cranial/caudal axis respiratory movement of the tumor. We verified all 10 breathing phases on 4DCT in cases 2 and 6. The range in Dice similarity index values was 0.78 to 0.86 for case 2 and 0.83 to 0.88 for case 6.

With the manual contour central coordinate as reference, the mean distance to the warped contour central coordinate in cases 2 and 6 was 0.03 cm and 0.04 cm, respectively, on the left/right axis, 0.07 cm and 0.06 cm on the anterior/posterior axis, and 0.06 cm and 0.07 cm on the cranial/caudal axis. For all 3 axes, the difference in central coordinates between the warped and manual contours was 0.2 cm or less during all breathing phases for cases 2 and 6.

Discussion

Previous studies reported that when performing SBRT to treat early-stage primary lung cancer, evaluation of ITV dose calculated for one phase on 4DCT could replace evaluation with GTV dose calculated by dose accumulation on 4DCT. Guckenberger et al compared ITV doses calculated for one phase of 4DCT and GTV doses calculated by dose accumulation for all breathing phases on 4DCT.[21] To compare these results with past reports, the dose was compared after being converted to the biological effective dose (BED) using the following formula for lung cancer: $\alpha/\beta=10$ Gy, and minimal dose received by 99% of the target volume was considered as the treatment dose: BED=dose/fraction × fraction number (1 + fraction dose/[α/β]).[29, 30] Furthermore, the dose prescription was calculated for 2 patterns, *i.e.*, with 37.5 Gy/3 fr to the PTV enclosure the 65% isodose (PTV 65%) and 80% isodose (PTV 80%). They reported that the ITV doses calculated for one phase of 4DCT with BED conversion were 135.1 ± 10.1 Gy and 104.6 ± 4.4 Gy for PTV −65% and PTV −80%, respectively, and that the GTV doses calculated by dose accumulation on 4DCT were 143.0 ± 8.2 Gy and 106.6 ± 3.8 Gy for PTV −65% and PTV −80%, respectively.[21] For PTV= ITV, Admiraal et al used a dose prescription of 60 Gy for 95% of the PTV and 54 Gy for 99% of the PTV. They reported that the minimum dose distributed in 99% of volume (D99) was a mean of 58.1 Gy for the ITV dose calculated on average for 4DCT, and a mean of 58.7 Gy for the CTV dose calculated by accumulating doses for all breathing phases on 4DCT.[22] Matsugi et al investigated ITV dose calculated on average for 4DCT, and GTV dose was calculated by accumulating doses for all breathing phases of 4 DCT. They reported that the mean differences between the ITV and GTV for D99, D95, and the minimum dose distributed in 1% of volume (D1) were −1.1%, −1.1%, and

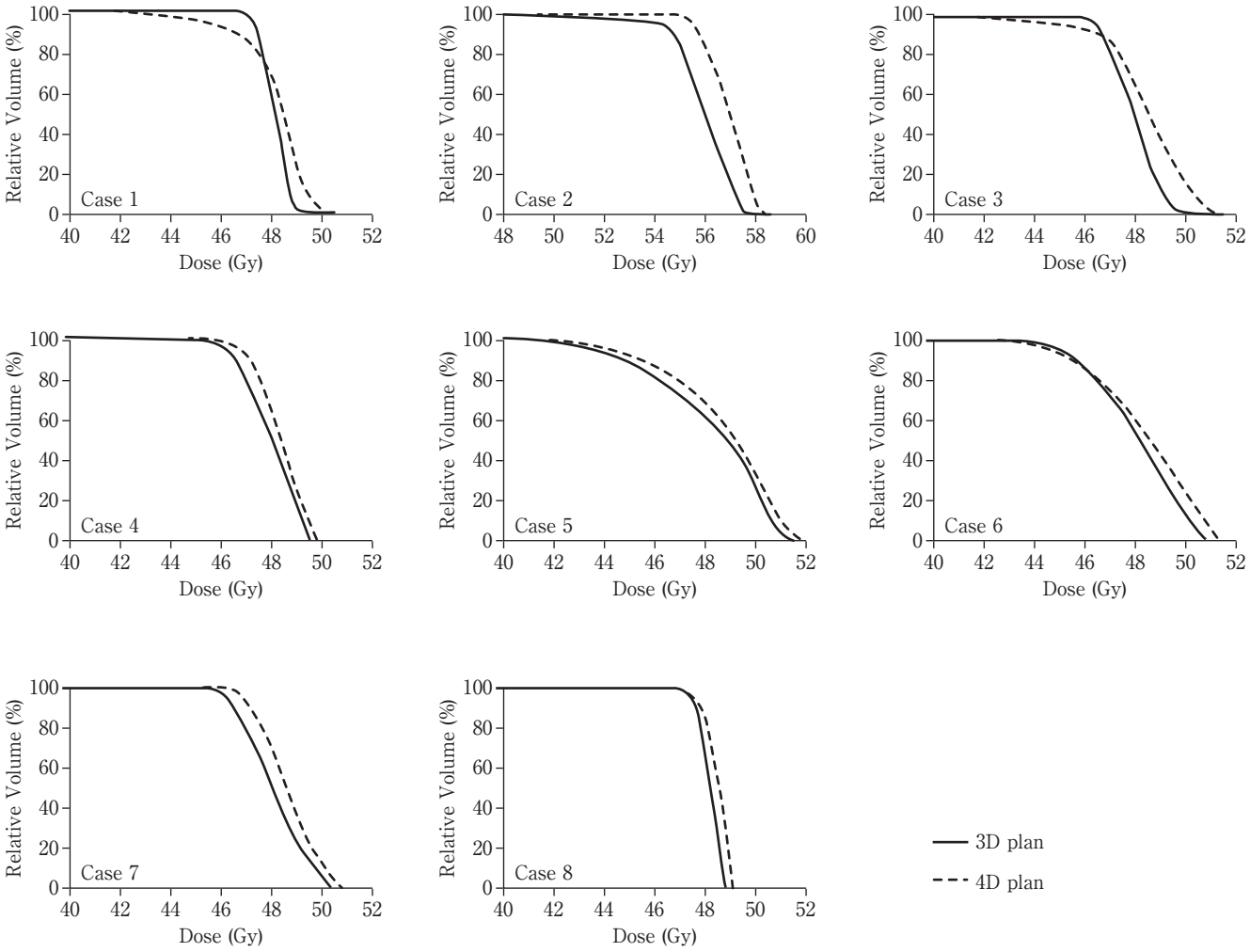

Fig. 2 High dose end of the DVH for ITV in all patients. Solid lines indicate 3D plans, and dotted lines indicate 4D plans.
DVH: dose-volume histogram, ITV: internal target volume, 3D: three-dimensional, 4D: four-dimensional

−0.1%, respectively.[23]

In this study, we confirmed that when dose prescription was performed using mean ITV dose on 3DCT for SBRT treatment of early-stage lung cancer, mean ITV dose calculated with a 4D plan was identical to or greater than that calculated with a 3D plan (Table 3, Fig. 1). In the JCOG-0403, the HI of a PTV dose below 1.6 was considered appropriate.[31, 32] Although there are no clear rules for appropriate HI standards for ITV dose, past case reports found that the mean HI of ITV dose ranges from 1.14 to 1.20 in SBRT.[21, 23] We did not observe any marked decreases in dose uniformity, as the mean HI was 1.15 (range: 1.06–1.31) for the 3D plans and 1.18 (range: 1.07–1.33) for the 4D plans. Using 4DCT for dose calculation, we confirmed that the intended doses were applied to the ITV after treatment planning using 3DCT.

Past studies also reported decreased doses in the PTV margins. Evaluation of PTV dose in 3D plans is not thought to be a suitable substitute for evaluation with GTV dose and CTV dose calculated by accumulating doses on 4DCT.[21, 23] In lung cancer therapy, the PTV margin contains many normal lung shadows surrounding the tumor. Dose distribution in the normal lung area is lower than in the tumor shadow, because CT density is lower for normal lung areas than for tumor shadows. This may partially explain why PTV doses were lower in the margin. Because ITV is essentially CTV with the addition of internal margins to account for physiological movement, it is likely that the 4D plan ITV margin dose, or doses in low-dose areas such as the ITV minimum dose, D98, and D95, would be lower than those of the 4D plan GTV and CTV. In the present analysis of ITV dose D2, mean dose, D95,

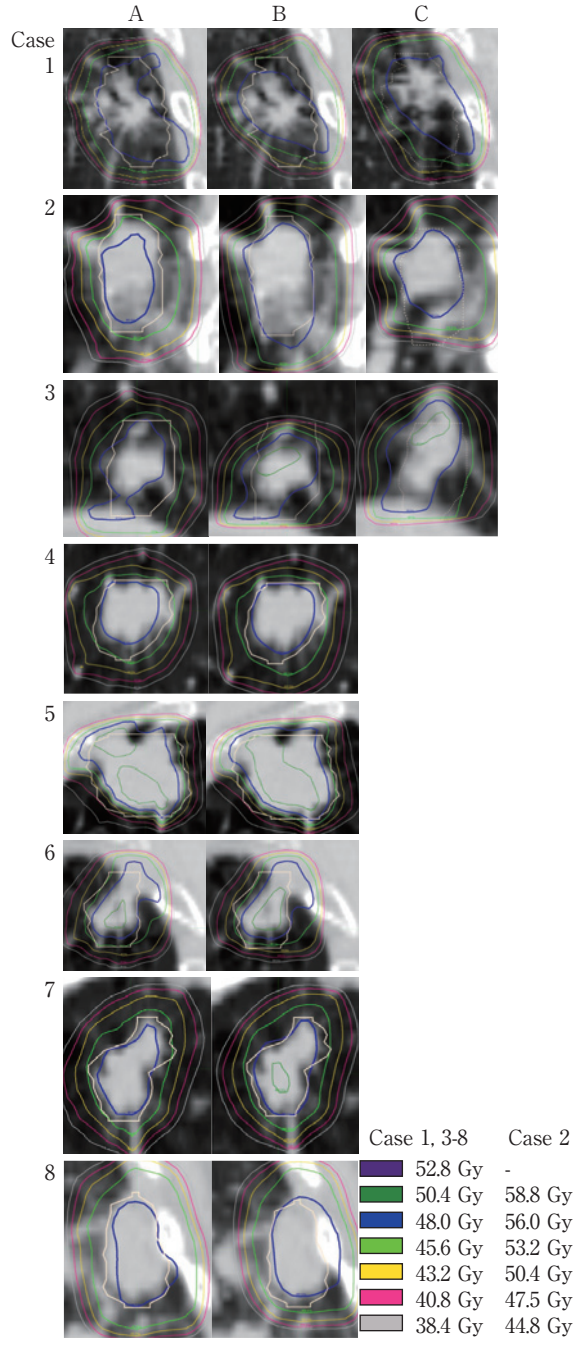

Fig. 3 Dose distribution for the 8 patients. All CT images are coronal views.
A: 3D plan
B: 4D plan with dose accumulation by DIR using 3DCT as the primary CT
C: 4D plan with dose accumulation by DIR using maximum expiration-phase 4DCT as the primary CT. White lines indicate ITV on 3DCT.
CT: computed tomography, 3D: three-dimensional, 4D: four-dimensional, DIR: deformable image registration, ITV: internal target volume

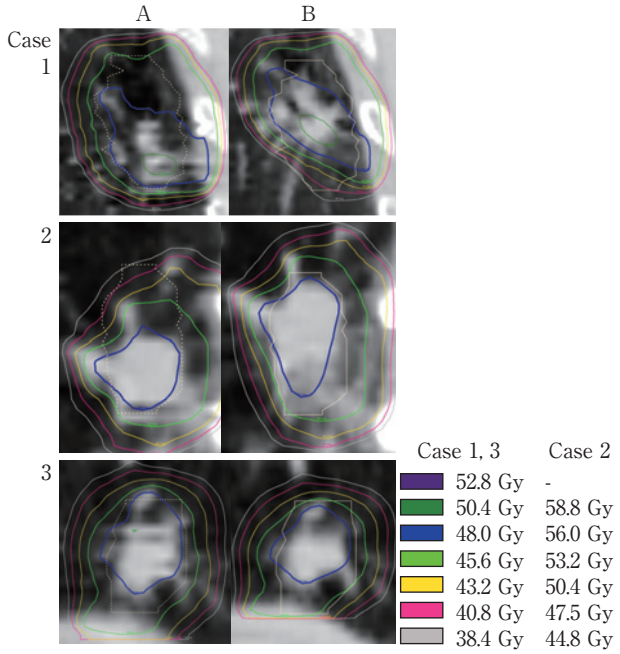

Fig. 4 Dose distributions for cases 1 through 3. All CT images are coronal views.
A: Dose distribution during 4DCT maximum inspiration-phase
B: Dose distribution on 3DCT registered from dose distribution during maximum inspiration-phase 4DCT image using DIR. White lines indicate ITV contours on 3DCT. Areas transferred onto 4DCT images from ITV contours on 3DCT and by parallel movement only are shown by the white dotted lines.
CT: computed tomography, 3D: three-dimensional, 4D: four-dimensional, ITV: internal target volume, DIR: deformable image registration

and D98, we observed large discrepancies between 3D and 4D plans for D98 and D95, where low doses were observed (Fig. 1). D98 and D95 are thought to reflect doses in the ITV margins. Large differences were noted between the plans for D98 and D95 in cases 1 through 3 (Table 3). In the 4D plans, DVH and isodose curve shapes deviated from those in 3D plans for cases 1 through 3 (Fig. 2, 3).

Of the 8 patients, cases 1 through 3 exhibited large tumor respiratory movement (≥0.9 cm). We compared tumor shadows on 4DCT and 3DCT for cases 1 through 3 and found that tumor shadows were identical on 3DCT and 4DCT for case 1, larger on 3DCT than on 4DCT for case 2, and smaller on 3DCT than on 4DCT for case 3 (Fig. 5). In this study, 3DCT performed during treatment planning was conducted in a free-breathing state. When 3DCT is performed under such conditions, motion artifacts and

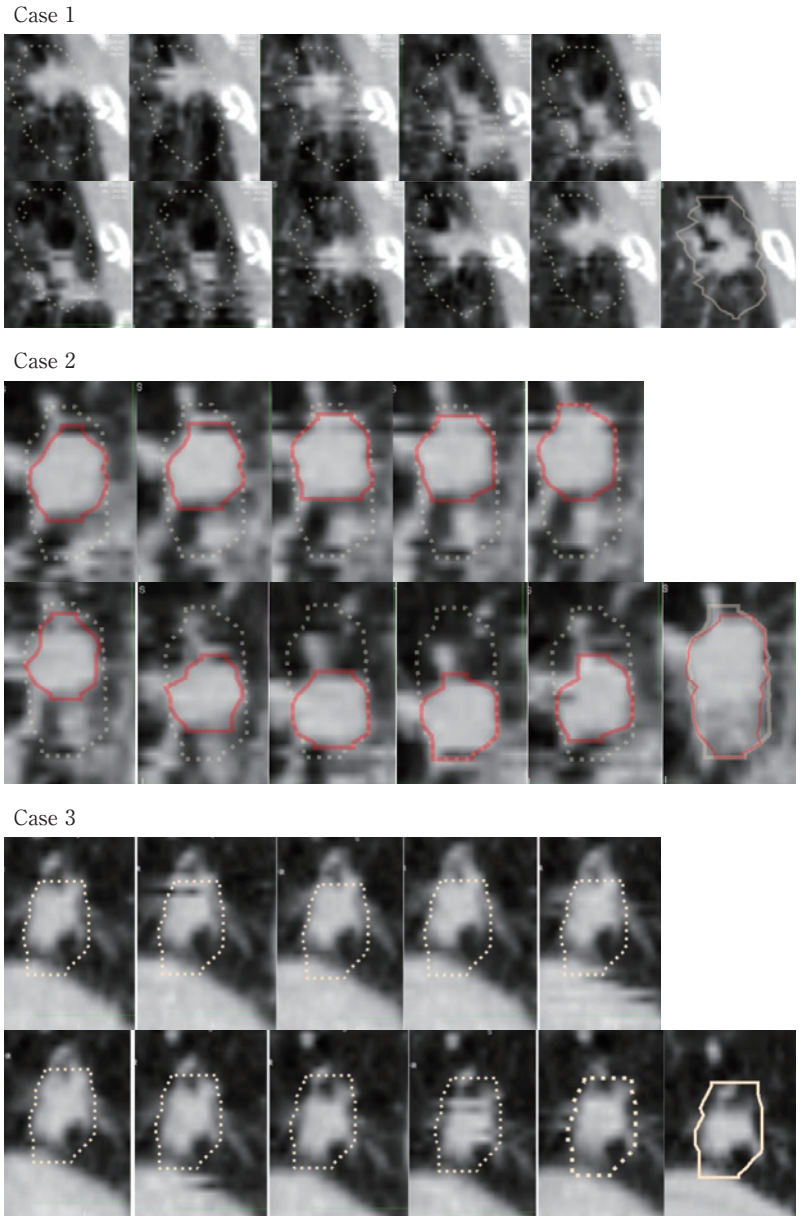

Fig. 5 Differences between 3DCT and 4DCT for cases 1 through 3. The upper row shows 5, 15, 25, 35% and 45% of 4DCT, in order, from the left side. The lower row shows 55, 65, 75, 85% and 95% of 4DCT, in order, from the left side. The rightmost image on the lower row shows 3DCT. All CT images are coronal views. The white lines indicate ITV contours. The red lines in case 2 indicate the CTV for each phase.
3D: three-dimensional, CT: computed tomography, 4D: four-dimensional, ITV: internal target volume, CTV: clinical target volume

tumor deformation (from tumor movement) are captured differently by imaging timing. Tumor shadows may thus expand or contract. This explains why the tumor shadows in cases 1 through 3 exhibited irregular expansion and contraction in the comparison of 4DCT and 3DCT.

The DIR that we used for dose accumulation was intensity-based. DIR was performed in accordance with contrast between voxels on CT. When DIR for only one phase was performed, the isodose curve changed to follow the movement of the high-attenuation areas on the pri-

mary CT (Fig. 4). We believe that when 4D dose accumulation using DIR is performed, the high-dose distribution area will shift in accordance with the high-density area, *i.e.*, the tumor.

In the 4D plans for cases 1 through 3, the isodose curves of prescribed doses changed in shape in accordance with the areas of high density on the primary CT (Fig. 3). In cases 1 and 3, the size of tumor shadows on 3DCT was identical to that observed on 4DCT, or only slightly smaller. Furthermore, in cases 1 and 3, the tumor movement accompanying respiration confirmed on 4DCT was more prominent. In cases 1 and 3, when dose accumulation was conducted with 3DCT as the primary CT, DIR was implemented in accordance with the movement of the tumor shadow accompanying respiration. The large deformation observed in prescription dose–level isodose curves may have reduced D95 and D98 on the 4D plans. In case 2, 3DCT tumor shadows were larger than those observed for each breathing phase on 4DCT (Fig. 5). In the dose accumulation for case 2, DIR was implemented in accordance with the tumor shadows on 3DCT, which were larger than those on 4DCT. In addition, the prescription dose–level isodose curves were more expanded with the 4D plan than with 3D plan. This expansion of prescription dose–level isodose curves may explain why the 4D plan doses increased overall. In cases 1 through 3, when dose accumulation was carried out using 4DCT as the primary CT, the isodose curve shape of the prescription dose changed from that obtained using 3DCT as the primary CT (Fig. 3C). Thus, it appears that differences in tumor shadows between the registration CT and the primary CT affect 4D dose accumulation with DIR. We believe that the selection of primary CT for dose accumulation is very important in using a 4D plan with DIR to evaluate dose distribution of a 3D plan when there is substantial respiratory movement of the tumor.

Limitations

We conducted dose calculation on 4DCT using supplemental data outside the imaging range of 3DCT. Areas of uncertainty resulting from the use of these supplemental data could cause errors in dose evaluation. Furthermore, we did not evaluate variables other than respiratory movement. In particular, because we did not consider setup error during treatment or patient movement during irradiation in our analysis, the present results may differ from those for the actual dose distribution.

Verification of DIR precision

DIR precision verification can be difficult because no standards for differences in contour central coordinates or similarity index standards have been established. In a previous study, the Dice similarity index was used for DIR precision verification, and a result of at least 0.8 was considered to indicate good precision.[33, 34] Our Dice similarity index results indicated good similarity, with ranges of 0.78 to 0.86 and 0.83 to 0.88 for cases 2 and 6, respectively. The mean distance to the warped contour central coordinate from the manual contour central coordinate (the reference) in cases 2 and 6 was 0.03 cm and 0.04 cm, respectively, on the left/right axis, 0.07 cm and 0.06 cm on the anterior/posterior axis, and 0.06 cm and 0.07 cm on the cranial/caudal axis. For all axes, differences between central coordinates were 0.2 cm or less. The thickness of the 4DCT slice in this study was 0.2 cm. Therefore, for all axes in cases 2 and 6, the difference between the center coordinate was smaller than or equal to the slice thickness of the 4DCT. Although some previous reports have measured differences in contour central coordinates to verify DIR precision, none have demonstrated clear standards for precision.[25, 35, 36] Brock et al gathered data from multiple facilities that had verified DIR precision for lung CT. They reported that the range of the distance to the warped contour central coordinate (using the manual contour central coordinate as a reference) was 0.06 to 0.12 cm on the left/right axis, 0.05 to 0.18 cm on the anterior/posterior axis, and 0.07 to 0.20 cm on the cranial/caudal axis.[25] Thus, we do not believe that there were any serious problems with DIR precision in our study, as the central coordinate errors were within these ranges.

Conclusion

Using 4DCT for dose calculation, we confirmed that the intended doses were applied to the ITV by treatment planning using 3DCT. However, differences might occur between 3D and 4D plans in parameters thought to reflect doses in the ITV margins, and total dose distribution changed in patients with large respiratory movement of tumors. In 4D dose accumulation using DIR, the dose distribution changed when the primary CT was changed, perhaps because of differences in tumor shadows between 3DCT and 4DCT. When using 4D plans with DIR to evaluate the dose distribution of 3D plans, the selection of primary CT for dose accumulation is important.

We thank Yuuki Miyabe MD of Kyoto University, for his valuable advice regarding the manuscript.

Conflicts of interest: The authors declare that they have no conflicts of interest regarding this work. This study was performed without the aid of a research grant.

References

1) Nakagawa T, Negoro Y, Matsuoka T, Okumura N, Dodo Y. Comparison of the outcomes of stereotactic body radiotherapy and surgery in elderly patients with cT1-2N0M0 non-small cell lung cancer. Respir Investig. 2014; 52: 221-6.
2) Onishi H, Shirato H, Nagata Y, Hiraoka M, Fujino M, Gomi K, et al. Stereotactic body radiotherapy (SBRT) for operable stage I non-small-cell lung cancer: can SBRT be comparable to surgery? Int J Radiat Oncol Biol Phys. 2011; 81: 1352-8.
3) Grills IS, Mangona VS, Welsh R, Chmielewski G, Mclnerney E, Martin S, et al. Outcomes after stereotactic lung radiotherapy or wedge resection for stage I non-small-cell lung cancer. J Clin Oncol. 2010; 28: 928-35.
4) Crabtree TD, Denlinger CE, Meyers BF, El Naqa I, Zoole J, Krupnick AS, et al. Stereotactic body radiation therapy versus surgical resection for stage I non-small cell lung cancer. J Thorac Cardiovasc Surg. 2010; 140: 377-86.
5) Jeppesen SS, Schytte T, Jensen HR, Brink C, Hansen O. Stereotactic body radiation therapy versus conventional radiation therapy in patients with early stage non-small cell lung cancer: an updated retrospective study on local failure and survival rates. Acta Oncol. 2013; 52: 1552-8.
6) Nagata Y, Hiraoka M, Shibata T, Onishi H, Kokubo M, Karasawa K, et al. Prospective trial of stereotactic body radiation therapy for both operable and inoperable T1N0M0 non-small cell lung cancer: Japan Clinical Oncology Group Study JCOG0403. Int J Radiat Oncol Biol Phys. 2015; 93: 989-96.
7) Keall PJ, Mageras GS, Balter JM, Emery RS, Forster KM, Jiang SB, et al. The management of respiratory motion in radiation oncology report of AAPM Task Group 76. Med Phys. 2006; 33: 3874-900.
8) Shirato H, Seppenwoolde Y, Kitamura K, Onimura R, Shimizu S. Intrafractional tumor motion: lung and liver. Semin Radiat Oncol. 2004; 14: 10-8.
9) Matsuo Y, Onishi H, Nakagawa K, Nakamura M, Ariji T, Kumazaki Y, et al. Guidelines for respiratory motion management in radiation therapy. J Radiat Res. 2013; 54: 561-8.
10) Stevens CW, Munden RF, Forster KM, Kelly JF, Liao Z, Starkschall G, et al. Respiratory-driven lung tumor motion is independent of tumor size, tumor location, and pulmonary function. Int J Radiat Oncol Biol Phys. 2001; 51: 62-8.
11) van Sörnsen de Koste JR, Lagerwaard FJ, Nijssen-Visser MR, Graveland WJ, Senan S. Tumor location cannot predict the mobility of lung tumors: a 3D analysis of data generated from multiple CT scans. Int J Radiat Oncol Biol Phys. 2003; 56: 348-54.
12) Sixel KE, Ruschin M, Tirona R, Cheung PC. Digital fluoroscopy to quantify lung tumor motion: potential for patient-specific planning target volumes. Int J Radiat Oncol Biol Phys. 2003; 57: 717-23.
13) International Commission on Radiation Units and Measurements. Prescribing, recording, and reporting photon beam therapy (Report 62) ICRU: Bethesda (MD); 1998.
14) Underberg RW, Lagerwaard FJ, Cuijpers JP, Slotman BJ, van Sörnsen de Koste JR, Senan S. Four-dimensional CT scans for treatment planning in stereotactic radiotherapy for stage I lung cancer. Int J Radiat Oncol Biol Phys. 2004; 60: 1283-90.
15) Vedam SS, Keall PJ, Kini VR, Mostafavi H, Shukla HP, Mohan R. Acquiring a four-dimensional computed tomography dataset using an external respiratory signal. Phys Med Biol. 2003; 48: 45-62.
16) Ehrhardt J, Lorenz C, editors. 4D modeling and estimation of respiratory motion for radiation therapy. Berlin: Springer; 2013.
17) Underberg RW, Lagerwaard FJ, Slotman BJ, Cuijpers JP, Senan S. Use of maximum intensity projections (MIP) for target volume generation in 4DCT scans for lung cancer. Int J Radiat Oncol Biol Phys. 2005; 63: 253-60.
18) Rietzel E, Chen GT, Choi NC, Willet CG. Four-dimensional image-based treatment planning: target volume segmentation and dose calculation in the presence of respiratory motion. Int J Radiat Oncol Biol Phys. 2005; 61: 1535-50.
19) Keall PJ, Joshi S, Vedam SS, Siebers JV, Kini VR, Mohan R. Four-dimensional radiotherapy planning for DMLC-based respiratory motion tracking. Med Phys. 2005; 32: 942-51.
20) Keall P. 4-Dimensional computed tomography imaging and treatment planning. Semin Radiat Oncol. 2004; 14: 81-90.
21) Guckenberger M, Wilbert J, Krieger T, Richter A, Baier K, Meyer J, et al. Four-dimensional treatment planning for stereotactic body radiotherapy. Int J Radiat Oncol Biol Phys. 2007; 69: 276-85.
22) Admiraal MA, Schuring D, Hurkmans CW. Dose calculations accounting for breathing motion in stereotactic lung radiotherapy based on 4D-CT and the internal target volume. Radiother Oncol. 2008; 86: 55-60.
23) Matsugi K, Nakamura M, Miyabe Y, Yamauchi C, Matsuo Y, Mizowaki T, et al. Evaluation of 4D dose to a moving target with Monte Carlo dose calculation in stereotactic body radiotherapy for lung cancer. Radiol Phys Technol. 2013; 6: 233-40.
24) Kashani R, Hub M, Balter JM, Kessler ML, Dong L, Zhang L, et al. Objective assessment of deformable image registration in radiotherapy: a multi-institution study. Med Phys. 2008; 35: 5944-53.
25) Brock KK; Deformable Registration Accuracy Consortium. Results of a multi-institution deformable registration accuracy study (MIDRAS). Int J Radiat Oncol Biol Phys. 2010; 76: 583-96.
26) Kirby N, Chuang C, Ueda U, Pouliot J. The need for application-based adaptation of deformable image registration. Med Phys. 2013; 40: 011702.
27) Balik S, Weiss E, Jan N, Roman N, Sleeman WC, Fatyga M, et al. Evaluation of 4-dimensional computed tomography to 4-dimensional cone-beam computed tomography deformable image registration for lung cancer adaptive radiation therapy. Int J Radiat Oncol Biol Phys. 2013; 86: 372-9.
28) Dice LR. Measures of the amount of ecologic association between species. Ecology. 1945; 26: 297-302.
29) Wulf J, Baier K, Mueller G, Flentje MP. Dose-response in stereotactic irradiation of lung tumors. Radiother Oncol. 2005; 77: 83-7.
30) Onishi H, Araki T, Shirato H, Nagata Y, Hiraoka M, Gomi K, et al. Stereotactic hypofractionated high-dose irradiation for stage I nonsmall cell lung carcinoma: clinical outcomes in 245 subjects in a Japanese multiinstitutional study. Cancer. 2004; 101: 1623-31.
31) Matsuo Y, Takayama K, Nagata Y, Kunieda E, Tateoka K, Ishi-

zuka N, et al. Interinstitutional variations in planning for stereotactic body radiation therapy for lung cancer. Int J Radiat Oncol Biol Phys. 2007; 68: 416-25.
32) Nishio T, Kunieda E, Shirato H, Ishikura S, Onishi H, Tateoka K, et al. Dosimetric verification in participating institutions in a stereotactic body radiotherapy trial for stage I non-small cell lung cancer: Japan clinical oncology group trial (JCOG0403). Phys Med Biol. 2006; 51: 5409-17.
33) Mattiucci GC, Boldrini L, Chiloiro G, D'Agostino GR, Chiesa S, De Rose F, et al. Automatic delineation for replanning in nasopharynx radiotherapy: what is the agreement among experts to be considered as benchmark? Acta Oncol. 2013; 52: 1417-22.
34) Chao KS, Bhide S, Chen H, Asper J, Bush S, Franklin G, et al. Reduce in variation and improve efficiency of target volume delineation by a computer-assisted system using a deformable image registration approach. Int J Radiat Oncol Biol phys. 2007; 68: 1512-21.
35) Gu X, Pan H, Liang Y, Castillo R, Yang D, Choi D, et al. Implementation and evaluation of various demons deformable image registration algorithms on a GPU. Phys Med Biol. 2010; 55: 207-19.
36) Kadoya N, Fujita Y, Katsuta Y, Dobashi S, Takeda K, Kishi K, et al. Evaluation of various deformable image registration algorithms for thoracic images. J Radiat Res. 2014; 55: 175-82.